Modeling high Re flow around a 2D cylindrical bluff body using the k-ω (SST) turbulence model.

A. L. J. Pang[1,2,*], M. Skote[2] and S. Y. Lim[3]

[1]ERI@N, Interdisciplinary Graduate School, Nanyang Technological University, 50 Nanyang Avenue, Singapore 639798, Singapore
[2]School of Mechanical and Aerospace Engineering, Nanyang Technological University, 50 Nanyang Avenue, Singapore 639798, Singapore
[3]School of Civil and Environmental Engineering, Nanyang Technological University, 50 Nanyang Avenue, Singapore 639798, Singapore

Email: PA0002EW@ntu.edu.sg
Email: MSKOTE@ntu.edu.sg
Email: CSYLIM@ntu.edu.sg

*Corresponding author

Abstract:

In this work, we analyze the ability for the k-ω (SST) model to accurately predict a high Reynolds number, Re, flow around a cylindrical bluff body, relative to other two-equation RANS models. We investigate the sensitivity of incorporating a curvature correction modification in the k-ω (SST) model to improve the limitation of the eddy-viscosity based models of capturing system rotation and streamline curvature for a flow around a cylinder. Finally, the ability for this turbulence model to capture the surface roughness of the cylinder is evaluated. Based on this work, we conclude that the k-ω (SST) model is superior to other two-equation RANS models and is able to capture the effects of surface roughness. The curvature correction modification to the k-ω (SST) model further improves this model.

***Keywords*:** Turbulence, RANS, two-equation model, k-ω model, k-ε model, Flow around cylinder, High Reynolds Number flow, Surface Roughness, Curvature Correction, FLUENT

Biographical notes

Andrew Li Jian Pang received his B.Eng (Hons) from Nanyang Technological University and is currently a Phd candidate in the Interdisciplinary Graduate School at the Nanyang Technological University in Singapore. His research interests are in the turbulence modeling, numerical sedimentation transport modeling and hydraulic engineering.

Martin Skote received his Master and Ph.D. degrees from the Royal Institute of Technology (KTH) in Stockholm, Sweden and is currently an Assistant Professor in the School of Mechanical & Aerospace Engineering at the Nanyang Technological University in Singapore. His research interest is in turbulent boundary layers, atmospheric flow, urban air quality and turbulence control modeling.

Siow Yong Lim received his Phd from the University of Liverpool and is currently an Associate Professor in the School of Civil and Environmental Engineering at the Nanyang Technological University in Singapore. His research interest is in sediment transportation engineering, water resources engineering and hydraulic/waterways engineering.

1. Introduction

Accurately modeling the flow around a cylindrical bluff body is critical in many engineering applications in order to determine the loads and mechanical responses of a structure. While there have been a significant amount of work done on such flows with lower Reynolds number, much less can be said for a higher Reynolds number flow regime. With marine structures, such as that of an offshore wind turbine foundation, scaling up in size in recent times, this understanding of high Reynolds number flow around a cylindrical bluff body is vital to ensure the reliability of such structures.

For the flow around a cylinder, earlier works have primarily relied on an empirical approach to understand such flows. While empirical studies have provided much insight, the physical size limitations of using an experimental approach have confined most of these earlier works to the lower Reynolds number flow regime. For high Reynolds number flows within the trans-critical regime, Schmidt (1966), Achenbach et al. (1968), Jones et al. (1969), James et al. (1980) and Schewe (1983) performed experimental work on the flow around a cylinder for Reynolds numbers of up to $\mathrm{Re} = 10^6$. These experimental work done derived key parameters including the coefficient of pressure (C_p), coefficient of drag (C_D), coefficient of lift root-mean-square (C_{Lrms}), angle of separation (θ) and the Strouhal number (St) for such a flow. However, due to the significant experimental challenges involved, minimal work has been done in the range around a Reynolds number of 10^7, with the highest Reynolds number of $\mathrm{Re} = 1.87 \times 10^7$ being obtained by Jones et al. (1969).

With the physical limitations of experimental work and with the advancement of computational capabilities in recent times, numerically modeling such a flow around a cylinder has become increasingly feasible and practical. This is especially so for high Reynolds number flows for

which fine grids are required to numerically model such flows. While theoretically a Direct Numerical Simulation (DNS) or a Large Eddy Simulation (LES) will provide the optimal solution to model such a flow, even with current computational power, the computational cost involved in such a simulation for high Reynolds number flow makes these models impractical, especially in industrial engineering applications.

A less computationally expensive approach to model the turbulent flow around a cylinder is that of a Reynolds-Averaged Navier-Stokes (RANS) approach. Two recent investigations by Catalano et al.(2003) and Ong et al.(2009) evaluated the ability of the standard k-ε model to predict the flow around a cylinder. Ong et al.(2009) concluded that the predicted flow using the standard k-ε model agrees reasonably well with that of experimental data up to a Reynolds number of $\mathrm{Re} = 3.6 \times 10^6$ and it is a reliable turbulence model for engineering design purposes. However, it was also highlighted by Ong et al.(2003) that there were some inaccuracies in this model due to the strong anisotropy of the turbulence in such a flow around a bluff body. Unal and Goren (2005) did a comparative study of the one- and two- equation RANS model (Spalart Allmaras, k-ε and k-ω models) applied to the flow around a cylinder in the sub-critical flow range ($\mathrm{Re} = 10^4$) and concluded that the k-ω (SST) model correlates best with experimental observations.

While these earlier works have provided much insight into the flow mechanism and characteristics, there still remain many unanswered questions. For a trans-critical flow, how does the k-ω (SST) model perform relative to the other RANS models? Is the k-ω (SST) model improved when a curvature correction modification is incorporated? Is the k-ω (SST) model able to accurately capture the effect of surface roughness for such a flow? By providing insight to

these questions, we aim to provide engineers with greater confidence when modeling a high Reynolds number flow around a cylindrical bluff body.

Hence in this work, the objective is to determine the ability of the k-ω (SST) model to accurately predict a high Reynolds number turbulence flow around a cylindrical bluff body. We first conduct a comparative study between the k-ω (SST) and other two-equation RANS models to benchmark the k-ω (SST) performance with both experimental observations as well as other equivalent turbulence models results. We subsequently study the effects of incorporating a curvature corrections modification into the k-ω (SST) model. Finally, we vary the surface roughness of the cylinder to determine the ability of the k-ω (SST) model to capture the surface roughness effects. This article is an extension of a conference paper (Pang et al., 2013) entitled "Turbulence modeling around extremely large cylindrical bluff bodies" presented at the 23rd International Ocean and Polar Engineering Conference at Anchorage, Alaska from the 30 June – 5 July 2013.

2. Numerical Model

For the RANS approach, when the Reynolds decomposition model is substituted into the Navier Stokes equation, the resultant continuity and momentum equations are as follows:

$$\frac{\partial u_i}{\partial x_i} = 0 \tag{1}$$

$$\rho\left(\frac{\partial u_i}{\partial t} + \frac{\partial u_i u_j}{\partial x_j}\right) = -\frac{\partial p}{\partial x_i} + \frac{\partial}{\partial x_i}\left(\mu\left(\frac{\partial \mu_i}{\partial x_j} + \frac{\partial u_j}{\partial x_i} - \frac{2}{3}\delta_{ij}\frac{\partial u_l}{\partial x_l}\right)\right) + \frac{\partial}{\partial x_j}\left(-\rho\overline{u_i' u_j'}\right) \tag{2}$$

where u_i and u_j are the mean velocities, $u_i^{'}$ and $u_j^{'}$ are the fluctuating part of the velocity, p is the dynamic pressure, δ_{ij} is the kronecker delta and ρ is the density of fluid. These equations contain an unknown Reynolds stress ($-\rho\overline{u_i^{'}u_j^{'}}$) term, resulting in these equations being open. One approach to close the equations is to use the Boussinesq approximation, defined as:

$$-\rho\overline{u_i^{'}u_j^{'}} = \mu_t\left(\frac{\partial u_i}{\partial x_j}+\frac{\partial u_j}{\partial x_i}\right)-\frac{2}{3}\left(\rho k+\mu_t\frac{\partial u_k}{\partial x_k}\right)\delta_{ij} \tag{3}$$

where μ_t is the turbulent viscosity and k is the turbulence kinetic energy. The turbulent viscosity (μ_t) can be obtained by solving additional transport equations. The number of additional transport equations that are needed depends on the turbulence model chosen. In this work, the focus will be on the k-ω (SST) model and we will benchmark this model against other two-equation (k-ε model and k-ω models) turbulence models.

2.1 The k-ω (SST) model

The k-ω (SST) model (Menter, 1994) capitalizes on the accuracy of the k-ω model within the near-wall region and the k-ε model in the far-field region. Such an approach is done by transforming the k-ε model into a k-ω formulation and incorporating a blending function between the two regions. As such, the k-ω (SST) model is able to model a wide range of flow profiles with increased accuracy. The transport equations for the k-ω (SST) model are given as:

$$\frac{\partial}{\partial t}\left(\rho k\right)+\frac{\partial}{\partial x_i}\left(\rho k u_i\right)=\frac{\partial}{\partial x_j}\left[\Gamma_k\frac{\partial k}{\partial x_j}\right]+\tilde{G}_k-Y_k \tag{4}$$

$$\frac{\partial}{\partial t}(\rho\omega)+\frac{\partial}{\partial x_i}(\rho\omega u_i)=\frac{\partial}{\partial x_j}\left[\Gamma_\omega\frac{\partial\omega}{\partial x_j}\right]+G_\omega-Y_\omega+D_\omega \tag{5}$$

where $\tilde{G}_k$ and G_ω represent the production terms of k and ω, Y_k and Y_ω represent the dissipation terms of k and ω, Γ_k and Γ_ω represents the effective diffusivity of k and ω, and finally D_ω represents the cross-diffusion term. A blending function, F_1, between the near-wall and far-field region is embedded within the derivation of the production, dissipation, diffusivity and cross-diffusion terms as follows:

$$\phi=F_1\phi_1+(1-F_1)\phi_2 \tag{6}$$

where ϕ_1 represents any constants in the original k-ω model , ϕ_2 represents any constants in the transformed k-ε model, ϕ is the resultant constant of the model and F_1 is the blending function, which is 1 in the near was region and 0 far away from the surface. Details of the k-ω (SST) model and its blending function are described fully by Menter (1994).

A limitation of an eddy-viscosity based model is that these models are less sensitive to system rotation and streamline curvature. Hence, in order to correct for this limitation, a curvature correction was proposed by Smirnov and Menter (2009) which was based on a rotation-curvature correction suggested by Spalart and Shur (1997) earlier. In this curvature correction modification, a multiplier (f_{r1}) was incorporated into the production term of the k-ω (SST) model given by:

$$f_{r1}=\max\left\{\min\left(f_{rotation},1.25\right),0.0\right\} \tag{7}$$

with

$$f_{rotation} = (1 + c_{r1}) \frac{2r^*}{1 + r^*} \left[1 - c_{r3} \tan^{-1}\left(c_{r2} \tilde{r} \right) \right] - c_{r1} \tag{8}$$

where c_{r1}, c_{r2} and c_{r3} are empirical constants and r^* and $\tilde{r}$ are functions of vorticity and strain rate tensors. A limit was imposed on the multiplier, $0 \le f_{r1} \le 1.25$, to ensure numerical stability (for strong convex curvature, $f_{r1} = 0$) and to prevent over-generation of eddy viscosity in flow with destabilizing curvature (for strong concave curvature, $f_{r1} = 1.25$). This curvature correction modification is a standard option available in FLUENT 14.

To account for surface roughness during the fluid flow, the law of the wall can be modified by incorporating an additive constant, ΔB, into the log-law as given by:

$$\frac{U_p u^*}{\tau_w / \rho} = \frac{1}{\kappa} \ln\left(E \frac{u^* y_p}{\nu} \right) - \Delta B \tag{9}$$

where y_p and U_p are the height and velocity at the wall adjacent cell, u^* is the wall friction velocity defined as $u^* = C_\mu^{1/4} k^{1/2}$, τ_w is the wall shear stress, κ is the von Karman constant and E is an empirical constant.

While there is currently no universal roughness function, the derivation of ΔB can be determined based on the non-dimensional surface roughness height, K_s^+, defined as:

$$K_s^+ = \rho K_s u^* / \mu \tag{10}$$

where K_s is the physical roughness height. Based on the non-dimensional surface roughness height, K_s^+, Cebeci and Bradshaw (1977) proposed formulas for ΔB based on the surface roughness regime it is in:

Smooth Regime ($K_s^+ \le 2.25$)

$$\Delta B = 0 \tag{11}$$

Transitional Regime ($2.25 < K_s^+ \le 90$)

$$\Delta B = \frac{1}{\kappa}\ln\left[\frac{K_s^+ - 2.25}{87.75} + C_s K_s^+\right] \times \sin\left\{0.4258\left(\ln K_s^+ - 0.811\right)\right\} \tag{12}$$

Fully rough Regime ($K_s^+ > 90$)

$$\Delta B = \frac{1}{\kappa}\ln\left(1 + C_s K_s^+\right) \tag{13}$$

where C_s is the roughness constant.

2.2 The *k*-ε model

In addition to the *k*-ω model, the *k*-ε models is another popular two-equation turbulence model which utilizes the transport equations of the turbulence kinetic energy (*k*) and turbulence dissipation rate (ε). For the standard *k*-ε model (Launder and Spalding, 1972), it is a semi-empirical formula whereby the turbulence kinetic energy (*k*) was derived from an exact equation and the turbulence dissipation rate (ε) was determined using physical reasoning. The *k* and ε transport equations are given as:

$$\frac{\partial}{\partial t}(\rho k) + \frac{\partial}{\partial x_i}(\rho k u_i) = \frac{\partial}{\partial x_j}\left[\left(\mu + \frac{\mu_t}{\sigma_k}\right)\frac{\partial k}{\partial x_j}\right] + G_k + G_b - \rho\varepsilon - Y_M \tag{14}$$

$$\frac{\partial}{\partial t}(\rho \varepsilon) + \frac{\partial}{\partial x_i}(\rho \varepsilon u_i) = \frac{\partial}{\partial x_j}\left[\left(\mu + \frac{\mu_t}{\sigma_\varepsilon}\right)\frac{\partial \varepsilon}{\partial x_j}\right] + C_{1\varepsilon}\frac{\varepsilon}{k}\left(G_k + C_{3\varepsilon}G_b\right) - C_{2\varepsilon}\rho\frac{\varepsilon^2}{k} \tag{15}$$

where G_k and G_b represent the generation of turbulence kinetic energy, Y_M represents the contribution of the fluctuating dilatation in compressible turbulence to the overall dissipation rate, σ_k and σ_ε are the turbulence Prandtl numbers, and $C_{1\varepsilon}$, $C_{2\varepsilon}$ and $C_{3\varepsilon}$ are constants

Variations of the standard k-ε model are the RNG k-ε model and the realizable k-ε model. The RNG k-ε model (Yakhot and Orszag, 1986) was derived using the statistical renormalization group theory. As for the realizable k-ε model (Shih et al., 1995), it modified the turbulent viscosity formulation and also derived a new ε transport equation from an exact equation. These modifications enable the k-ε model to better capture the effects of swirling flow (RNG k-ε model) as well as flows with adverse pressure gradients and separation (realizable k-ε model).

As the k-ε model was developed for turbulent core flows, a wall function is needed to model the near wall regions. In this work, a standard wall function (Launder and Spalding, 1974) was used for all the k-ε model simulations performed.

3. Simulation

The simulation model was setup with the focus on understanding a high Reynolds flow around a practical engineering structure, in particular that of an offshore wind turbine monopile foundation. A cylindrical diameter of D = 4.2 m and the fluid input velocity of 1.25 m/s was used in the simulation model, replicating that experience by most of the offshore wind turbines foundations. This results in a high Reynolds number flow of Re = 5.2×10^6. The software FLUENT was used to perform all simulations due to its popularity among many engineers. All the simulations were done on a 2-D plane.

3.1 Model Geometrical Dimension and Mesh

The geometrical dimension of the computational domain used for all the simulations performed was 25D × 20D. From the center of the cylinder, the velocity inlet boundary was 10D upstream while the outflow boundary was 15D downstream from the center of the cylinder. The upper and lower far-field symmetrical boundaries were 10D from the center of the cylinder. This lateral distance chosen for the upper and lower far field is consistent with that proposed by Behr et al. (1994) whereby a distance of 8D or greater is recommended for flows around cylindrical bodies.

A hexahedral block mesh was used for all the simulations. The meshing of the model was divided into 2 zones, the inner zone, which is a 4D × 4D block around the cylinder, and the outer zone, which is the zone away from the cylinder. For the inner zone, the grid expansion ratio ranged from 1.01 – 1.05 from the cylinder wall. As for the outer zone, the grid expansion ratio from the inner zone edge was constant at 1.02 downstream and 1.05 for the upper and lower far fields and upstream direction. Figure 1 and Table 1 show the geometrical dimensions, meshing and boundary conditions of the computation domain used in the simulations. The Input Parameters defined in Table 1 describe the X-velocity component (u_x) and the Y-velocity components (u_y) respectively.

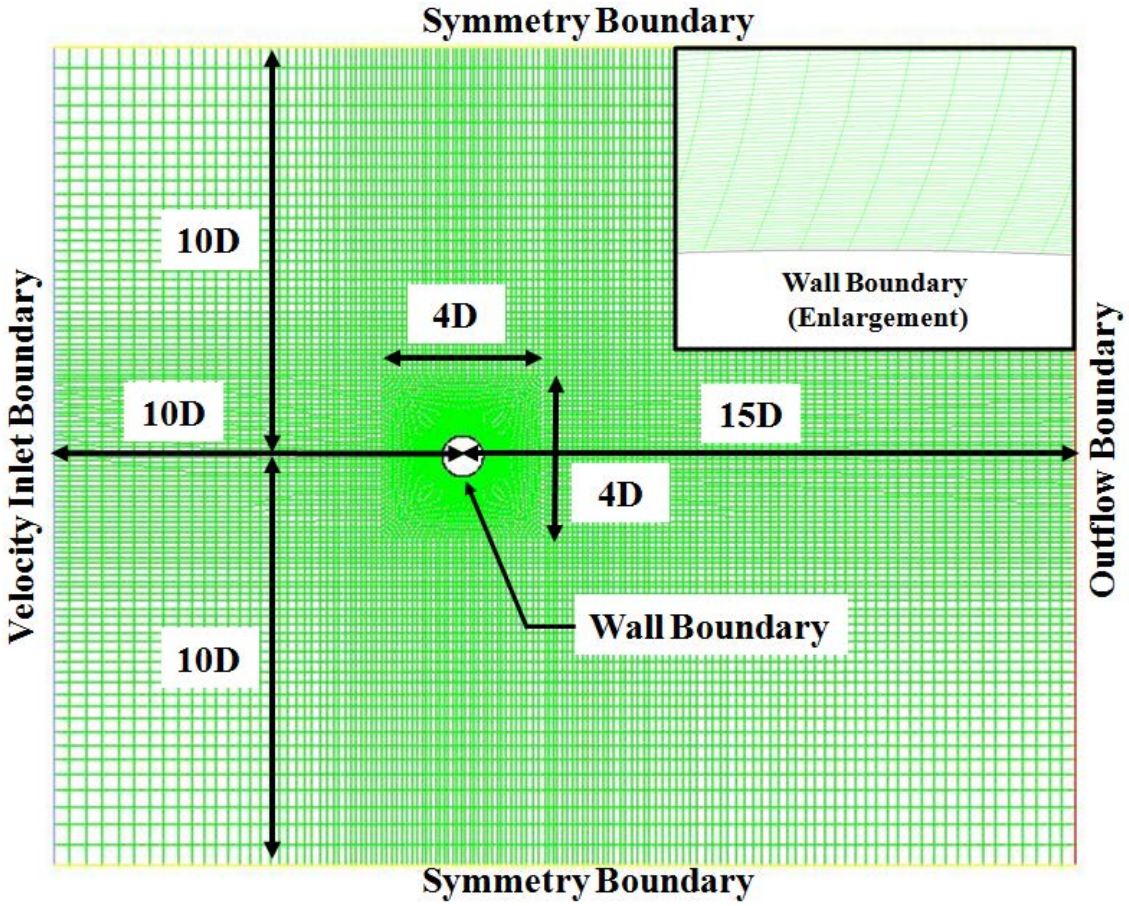

Figure 1 The geometrical dimensions and meshing of the computational domain used in the simulations.

Table 1 Boundary Conditions and input variables for the simulations performed in this work.

Zones	Boundary Conditions	Input Parameters
Upstream	Velocity Inlet	u_x=1.25 m/s, u_y=0 m/s
Downstream	Outflow	u_x=free, u_y=free
Upper and Lower Far-Field	Symmetry	u_x=free, u_y=0 m/s
Cylinder	Wall	u_x=0 m/s, u_y=0 m/s

3.2 Boundary Conditions and Input Parameters

For the inlet free stream flow, the input parameters were obtained from Jones *et al.* (1969) experiments whereby the turbulence intensity was I = 0.17%. The turbulence viscosity ratio, μ_t/μ = 1, which is recommended for external flows (FLUENT, 2013), was used in the simulations performed. The turbulent kinetic energy (k), turbulent dissipate rate (ε) and specific dissipation rate (ω) were determined as follows:

$$k = \frac{3}{2}\left(u_{avg} I\right)^2 \tag{16}$$

$$\varepsilon = \rho C_\mu \frac{k^2}{\mu}\left(\frac{\mu_t}{\mu}\right)^{-1} \tag{17}$$

$$\omega = \rho \frac{k}{\mu}\left(\frac{\mu_t}{\mu}\right)^{-1} \tag{18}$$

where u_{avg} is the mean velocity and C_μ = 0.09 is an empirical constant.

3.3 Numerical Scheme

A Finite Volume Method (FVM) approach was used to solve the governing equations. For the velocity-pressure coupling, a SIMPLE algorithm (Patankar and Spalding, 1972) was used while a second order upwind scheme (Barth and Jespersen, 1989) was used for the spatial discretization of the simulations done.

3.4 Mesh Sensitivity

A mesh sensitive study was done on each of the turbulence models used in the comparative study to ensure a grid independent solution was obtained for all the simulations. The percentage difference between the coefficient of drag (C_D), coefficient of lift root-mean-square value (C_{Lrms}) and Strouhal number (St) for the different grid sizes were less than 3% before a grid independence result was achieved.

Table 2 Results of the mesh sensitivity study for the k-ω *(SST)* model.

ID	Mesh Size (Elements)	C_D	Difference (%)	C_{Lrms}	Difference (%)	St	Difference (%)
M1	134900	0.508	10.03%	0.242	23.55%	0.305	5.25%
M2	227232	0.457	0.21%	0.185	2.16%	0.321	0.62%
M3	325244	0.458	-	0.181	-	0.323	-

Table 2 shows the results of the grid sensitivity study for the k-ω (SST) model. For M2 (227232 elements), increasing the mesh size by 43.13% to obtain M3 (325244 elements), a 0.21% variation in C_D, 2.16% variation in C_{Lrms}, and 0.62% variation in St was achieved. With this minor variation of C_D, C_{Lrms}, and St values with a significant increase in mesh size, it can be determined that a mesh independence solution was obtained for M2 and hence this mesh was used for the simulations performed.

4. RANS Comparative Study

To analyze the ability of the k-ω (SST) model to capture a trans-critical flow around a cylinder relative to other two-equation RANS models, a comparative study was performed between the k-ω (SST) and the k-ω (Standard) , k-ε (Standard) , k-ε (RNG) and k-ε (Realizable) models. The

key parameters used to evaluate each turbulence model are the coefficient of pressure-base (C_{pbase}), coefficient of drag (C_D), coefficient of lift root-mean-square (C_{Lrms}), angle of separation (θ) and the Strouhal number (St). These parameters are of significant interest in many practical engineering problems as they provide not only the key elements to predict the loading on a structure due to the fluid flow (C_{pbase}, C_D, C_{Lrms}), but also provide a good quantitative description of the flow patterns (θ, St) around the structure.

The coefficient of pressure-base (C_{pbase}) obtained from the simulation results are presented in Table 3, together with the experimental data. It is noted that a smooth cylinder was used in these simulations. When analyzing the pressure coefficient at the base of the cylinder (at angle 180°, C_{pbase}), it was observed that both the k-ω (SST) model and the k-ω (Standard) model correlated well with Jones et al.(1969) data of C_{pbase} = - 0.621. For the k-ε models, the simulations tend to under-predict the resultant base pressure, approximately C_{pbase} = - 0.37, as compared to experimental results which typically had a C_{pbase} value of greater than -0.60.

In addition to the coefficient of pressure-base (C_{pbase}), the angle of separation (θ), coefficient of drag (C_D), Strouhal number (St) and coefficient of lift-rms (C_{Lrms}) of the simulations were similarly obtained as shown in Table 3. The coupling between these parameters, as will be explained later, provides a good understanding and justification of the superior nature one turbulence model has over another when modeling a high Reynolds flow around a cylinder.

Table 3 The coefficient of pressure-base (C_{pbase}), angle of separation (θ), coefficient of drag (C_D), Strouhal number (St) and coefficient of lift-rms (C_{Lrms}) of the simulations results and experimental observations

Model	**Coeff. Of Pressure-base (C_{pbase})**	**Angle of Sep. (θ)**	**Coeff. Of Drag (C_D)**	**Strouhal number (St)**	**Coeff. Of Lift rms (C_{Lrms})**
k-ε (Standard)	-0.311	123.47	0.270	0.446	0.0744
k-ε (RNG)	-0.372	121.83	0.307	0.365	0.1702
k-ε (Realizable)	-0.385	122.38	0.313	0.426	0.0788
k-ω (Standard)	-0.594	114.70	0.463	0.320	0.4079
k-ω (SST)	-0.594	109.76	0.457	0.321	0.1847
Achenbach et al. (1968) Re=4.7×10^6	-	111.94	0.726	-	-
James *et al.* (1980) Re=5.46×10^6	-	110.94	0.317	0.229	-
Schmidt *et al.* (1966) Re=5.0×10^6	-0.605	-	0.533	-	0.1379
Roshko *et al.* (1961) Re=5.32×10^6	-0.853	-	0.697	0.263	-
Schewe (1983) Re=5.25×10^6	-	-	0.532	0.262	0.0467
Jones *et al.* (1969) Re=5.61×10^6	-0.621	-	0.636	0.253	0.1140

For the angle of separation, Table 3 shows that the k-ω (SST) model predicts the separation at θ=109.76°, which correlates well with Achenbach et al. (1968) and James et al. (1980). Similarly for the k-ω (standard) model, a reasonable agreement between the predicted θ and experimental data was observed, whereby we define a reasonable agreement of the simulations to be within a 25% deviation (generally within engineering tolerance) of that observed in experimental results. However, for all the k-ε models, the predicted angle of separation was significantly larger than the experimental data. For flow around a cylinder, the accurate modeling of the angle of separation is critical. This is because the width of the resultant leeward vortex shedding is highly dependent on the angle at which the flow separates. A smaller angle of separation will have a broader width of the leeward vortex shedding behind the cylinder and this results in a larger based pressure at the rear of the cylinder and a higher coefficient of drag. The vice-versa is similarly valid for larger angle of separations.

Hence, when analyzing the C_D obtained from the simulations, the good agreement using the k-ω (SST) model is due to the model's good prediction of the angle of separation (Table 3). For the k-ε model, the larger angle of separation predicted results in a narrower leeward vortex region, and hence a C_D which slightly under-predicts the smallest C_D obtained by James et al. (1980).

For the Strouhal number, both the k-ω and the k-ε models over-predicts the St number compared to that observed by experiments. However, the lower St number predicted by the k-ω models correlate better with experiments compared to the k-ε models. Again, this trend is attributed to the angle at which the flow separates. For larger angle of separation, the narrower leeward vortex increases the frequency of the vortex oscillations and hence an increase in the Strouhal number and vice-versa for smaller angle of separations.

For the coefficient of lift-rms value, Table 3 shows that the k-ε models have a better correlation with experimental data compared to the k-ω models, falling within the range of C_{Lrms} = 0.0467 - 0.1379 observed by Schewe et al. (1983) and Schmidt et al. (1966) respectively. The k-ω models tends to over-predict the C_{Lrms}. But the predicted C_{Lrms} value of the k-ω (SST) model agreed reasonably well with the results of Schmidt et al. (1966).

From the results obtained in the simulations, one may conclude that the k-ω (SST) model agreed best with experimental data for high Reynolds flow around a cylinder. The key parameter predicted well by the k-ω (SST) model is the angle at which the fluid separates around the cylinder, which resulted in good prediction of the C_D and the *St* number compared to the other two-equation RANS turbulence models. For the k-ε models, due to the larger angle of separation predicted, the resultant C_D and the *St* number did not agree well with the experimental data as compared to the k-ω (SST) model.

5. Curvature Correction and Surface Roughness

In the above discussions, a perfectly smooth cylinder was modeled for all the simulation presented. To provide more insights to the k-ω (SST) model, we extend the analysis to understand the effects of incorporating a curvature correction into the k-ω (SST) model, as well as to determine the ability of such a turbulence model in capturing the effects of the surface roughness of the cylinder. To the author's awareness, such an analysis on the curvature correction and surface roughness for flow profiles around a cylindrical bluff body has yet to be evaluated.

5.1 Curvature Correction

A weakness of the eddy-viscosity model is in capturing the effect of the flow curvature and rotation. To sensitize the turbulence model to account for such curvature, a multiplier, as described in the earlier section, is incorporated into the production term of the turbulence model. The C_p, C_{pbase}, C_D, C_{Lrms}, θ and St of the extended simulations are presented in Figure 2 and Table 4.

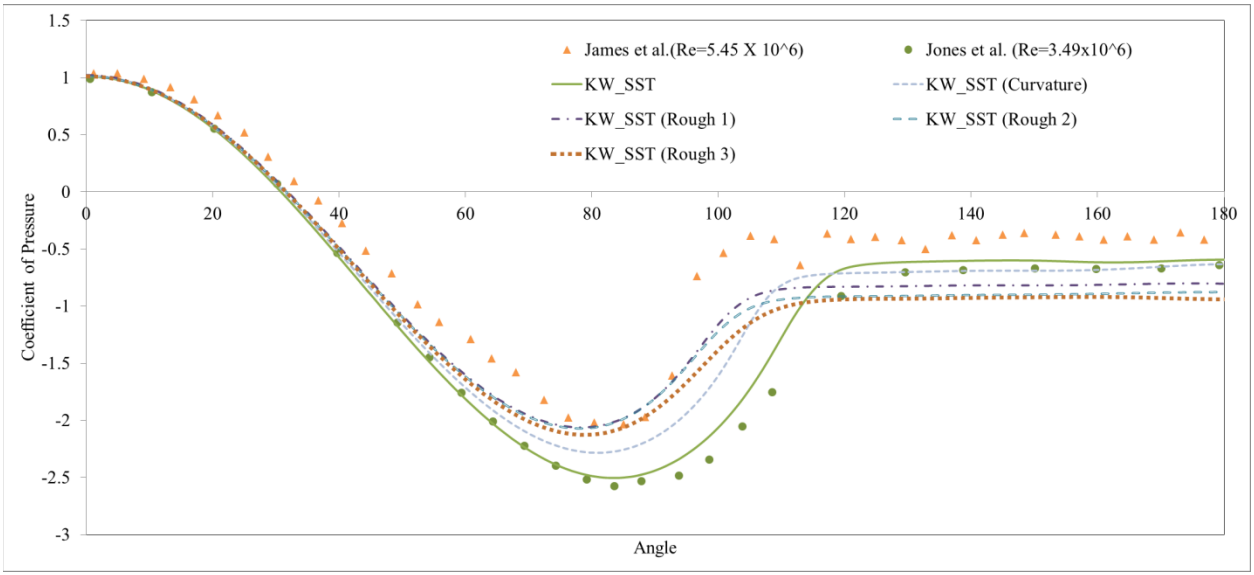

Figure 2 The coefficient of pressure (C_p) profile when a curvature correction modification and varying surface roughness are incorporated into the k-ω (SST) model

Table 4 The coefficient of pressure-base (C_{pbase}), coefficient of drag (C_D), coefficient of lift-rms (C_{Lrms}), angle of separation (θ) and strouhal number (St) when a curvature correction modification is incorporated into the k-ω (SST) model

		k-ω (SST) **Smooth**	k-ω (SST) with Curvature Correction **Smooth**
Coefficient of Pressure-Base	Simulations	-0.593	-0.632
	Experiments (Jones *et al.*, 1969)	-0.621	-0.621
Coefficient of Drag	Simulations	0.457	0.520
	Experiments (Jones *et al.*, 1969)	0.636	0.636
Coefficient of Lift (RMS)	Simulations	0.184	0.289
	Experiments (Jones *et al.*, 1969)	0.114	0.114
Angle of Separation	Simulations	109	109
	Experiments (James *et al.*, 1980)	110	110
Strouhal Number	Simulations	0.320	0.291
	Experiments (Jones *et al.*, 1969)	0.253	0.253

Figure 2 shows that when the curvature correction is activated, the coefficient of pressure profile is in closer agreement with James et al. (1980) as compared to the original k-ω (SST) turbulence model. Moving towards the rear of the cylinder (at angle 180°), the C_{pbase} of both the k-ω (SST) model (as seen in Table 4), with and without a curvature correction, approximately converges to that of $C_{pbase} \approx$ - 0.6.

The curvature correction causes both the coefficient of drag, C_D, and coefficient of lift-rms, C_{Lrms}, to increase. While the resultant C_D is closer to the experimental value observed by Jones *et*

al. (1969) as seen in Table 4, an increase in C_{Lrms} caused a larger discrepancy between the simulation and experimental results.

Table 4 shows that the curvature correction had minimal influence on the angle of separation. However, the curvature correction caused a decrease in the value of *St* (= 0.291), and hence a better agreement with experimental observations.

It may be concluded that the curvature correction does influence the predicted profiles and characteristics of a high Reynolds number flow around a cylinder. While omitting such a correction factor results in simulations that correlate reasonably well with experiments, it is beneficial to incorporate the curvature correction, which requires minimal additional computational cost, but improves the predicted C_p profile, C_D and *St* number.

5.2 Surface Roughness

For high Reynolds number flow around a cylinder, many researchers (Roshko, 1961, Jones et al., 1969, James et al., 1980) suggested that the surface roughness has a significant influence on the resultant flow parameters. Earlier experimental observations by Shih et al.(1993) and Achenbach (1971) on the effects of surface roughness for flows around a cylinder at high Reynolds number noted that an increase in the surface roughness was able to reduce the Reynolds number at which the transition between the flow regimes occurs.

To understand the ability for a k-ω (SST) model to capture the effect of surface roughness, we performed additional simulations. The K_s/D ratios used in these simulations were similar to the one used by Shih et al. (1993) as shown in Table 5.

Table 5 The roughness height, K_s/D ratio and roughness constant used in the simulations.

Model Name	Roughness Height / K_s (m)	K_s/D	Roughness Constant / C_s
k-ω_SST (Rough 1)	1.26×10^{-03}	3.00×10^{-4}	0.50
k-ω_SST (Rough 2)	5.04×10^{-03}	1.20×10^{-3}	0.50
k-ω_SST (Rough 3)	4.24×10^{-02}	1.01×10^{-2}	0.50

Table 6 The coefficient of pressure-base (C_{pbase}), coefficient of drag (C_D), coefficient of lift-rms (C_{Lrms}), angle of separation (θ) and strouhal number (St) when varying surface roughness are incorporated into the k-ω (SST) model

		k-ω (SST) **Rough 1**	k-ω (SST) **Rough 2**	k-ω (SST) **Rough 3**
Coefficient of Pressure (Base)	Simulations	-0.804	-0.876	-0.940
	Experiments (Shih *et al*., 1993)	-0.977	-1.049	-1.074
Coefficient of Drag	Simulations	0.705	0.768	0.806
	Experiments (Shih *et al*., 1993)	0.860	0.970	1.062
Coefficient of Lift (RMS)	Simulations	0.438	0.505	0.568
	Experiments (Shih *et al*., 1993)	NA	NA	NA
Angle of Separation	Simulations	108	110	109
	Experiments (Shih *et al*., 1993)	87	86	84
Strouhal Number	Simulations	0.261	0.258	0.267
	Experiments (Shih *et al*., 1993)	0.242	0.225	0.213

Figure 2 and Table 6 shows the simulation results with varying surface roughness, together with the experimental data obtained by Shih et al. (1993).

In Figure 2, it is shown that when the surface roughness (Rough 1, Rough 2 and Rough 3) is incorporated, the pressure profile around the upper and lower zones (at angle approx. 60° – 120°) of the cylinder decreases considerably, as expected with an increase in surface roughness. While the general relationship of the pressure profile with K_s/D is not so clear, the base pressure of the cylinder (at angle 180°), C_{pbase}, predicted by the k-ω (SST) model shows an inverse relationship with K_s/D, similar to the trend observed experimentally (Table 6). The k-ω (SST) model tends to slightly under-predict the C_{pbase}, but the simulation agrees reasonably well with the experiments of Shih et al. (1993). This is especially so as Shih et al. (1993) did highlight difficulties in obtaining the experimental data for $K_s/D = 3.00 \times 10^{-4}$ (Rough 1) and $K_s/D = 4.24 \times 10^{-02}$ (Rough 3) due to gaps in the cylinder/screen surface (Rough 1) and strong vibrations experienced by the cylinder (Rough 3) during the experiments.

Table 6 shows the results for the coefficient of drag. It can be seen that the k-ω (SST) model predicts an increasing trend of C_D with an increase in surface roughness similar to that observed in experiments. Although the magnitude of C_D obtained by the model tends to slightly underestimate that observed in experiments of Shih et al. (1993), the increasing C_D trend with higher surface roughness is clearly captured by the k-ω (SST) model. As for the coefficient of lift-rms, C_{Lrms} , the k-ω (SST) model predicts that C_{Lrms} increases with K_s/D ratio, as expected due to the added forces on the cylinder as a result of the surface roughness. Experimental results on C_{Lrms} are not available for comparison with our simulations.

Data from Shih et al. (1993) show that the angle of flow separation and Strouhal number is relatively insensitive to the K_s/D ratio, with a slight inverse relationship (Table 6). While it is noted that there is a constant magnitude difference between the simulation results and Shih et al. (1993) data, such a difference can be attributed to the challenges and difficulties in conducting a high Reynolds flow experiment. For a smooth cylinder, Shih et al. (1993) obtained a flow separation of $\theta = 98°$ which slightly differs from the value obtained in the present simulations, and also from that observed by Achenbach (1968) and James et al. (1980) of approximately $\theta = 111°$. Table 6 shows that the k-ω (SST) model captures the insensitivity of these parameters, which fluctuates slightly about a very narrow range of $\theta = 108°$ to $\theta = 110°$ and $St = 0.258$ to $St = 0.267$. Although the k-ω (SST) model is unable to predict the θ and St slight decreasing trend noted by Shih et al. (1993), the relative insensitivity of θ and St to the increase in K_s/D ratio is generally captured well by the k-ω (SST) model.

Hence, from the simulation results of the k-ω (SST) model, the evolution of the flow characteristic with increasing K_s/D can be captured reasonably well, for both the minor variation in angle of separation and Strouhal number, as well as the more substantial variation of the C_p and C_D with increasing surface roughness. While there are slight discrepancies in the magnitude of the parameters due to challenges of performing high Reynolds flow experiments, the ability of the k-ω (SST) model to capture the changes in flow parameter with K_s/D ratio is demonstrated.

7. Conclusion

In this work, we analyzed the ability for the k-ω (SST) model to capture the high Reynolds number flow around a cylindrical bluff body. Benchmarking the k-ω (SST) model against other two-equation RANS models, it was shown that the k-ω (SST) model had a closer agreement to experimental values as compared to other two-equation RANS turbulence models. This good agreement of the k-ω (SST) model with experimental data is due to the ability of this turbulence model to predict the angle of separation well, which corresponds to modeling the width of the leeward vortex wake, the Strouhal number and the coefficient of drag similarly well.

Advancing our analysis further, we studied the effects of incorporating a curvature correction modification into the k-ω (SST) model and determined the ability for this turbulence model to capture the surface roughness for a high Reynolds number flow. It was established that the curvature correction improved the coefficient of pressure profile while maintaining or slightly improving the predicted angle of separation, coefficient of drag and Strouhal number, which were already in good correlation with experimental data. However, the agreement of the coefficient of lift-rms with that of experimental value was worsened when the curvature correction was included. For the surface roughness analysis, the k-ω (SST) model was observed to be able to reasonably capture the flow characteristic evolution as the magnitude of the K_s/D ratio increases, especially so for the substantial variation of the C_p and C_D with increasing surface roughness. While there were minor discrepancies in the prediction of the angle of separation and strouhal number in the simulation results, the general trend of these flow parameters to vary minimally as the K_s/D ratio increases agreed well with that observed experimentally by Shih et al. (1993).

Hence, when selecting a two-equation RANS model for a high Reynolds number flow around a cylinder, the k-ω (SST) model, incorporating a curvature correction modification, best captures the flow characteristics and parameters of such a flow profile. In addition, given a variation in surface roughness of a cylinder, this turbulence model can reasonably capture the evolution of the flow characteristics as the magnitude of the K_s/D ratio increases. With the good correlation the k-ω (SST) model has with experimental observations, such a model can be applied to similar flow problems in practical engineering applications such as an offshore wind turbine monopile foundation.

Acknowledgement

The authors would like to acknowledge the support of the Energy Research Institute @ NTU (ERI@N) under the Offshore Renewable Joint Industry Programme (JIP) for their support in undertaking this work.

Reference

Achenbach, E. (1968) 'Distribution of local pressure and skin friction around a circular cylinder in cross-flow up to Re = 5×10^6', *J. Fluid Mech.,* Vol. 34**,** pp. 625-639.

Achenbach, E. (1971) 'Influence of surface roughness on the cross-flow around a circular cylinder', *J. Fluid Mech.,* Vol. 46**,** pp. 321-335.

ANSYS FLUENT (2011). ANSYS FLUENT User's Guide, ANSYS Inc. 2428 pp.

Barth, T.J. and Jespersen, D. (1989) 'The design and application of upwind schemes on unstructured meshes', *American Institute of Aeronautics and Astronautics,* Technical Report AIAA 89-0366.

Behr, M., Hastreiter, D., Mittal, S. and Tezduyar, T.E. (1994) 'Incompressible flow past a circular cylinder: Dependence of the computed flow field on the location of the lateral boundaries', *Comput. Meth. Appl. Mech. Eng.*, Vol. 123 pp. 309-316.

Catalano, P., Wang, M., Gianluca, I. and Parviz, M. (2003) 'Numerical simulation of the flow around a circular cylinder at high Reynolds numbers', *Int. J. Heat Fluid Fl.,* Vol. 24, pp. 463-469.

Cebeci, T. and Bradshaw, P. (1977) *Momentum transfer in boundary layers,* Hemisphere Publishing Corp., Washington, DC.

Unal, U.O. and Goren, O. (2005) 'Vortex shedding from a circular cylinder at high Reynolds number', *Proc. 11th Int. Congress of the Int. Maritime Assn. of the Mediterranean, Lisbon, Maritime Transportation and Exploitation of Ocean and Coastal Resources,* Vol. 2, pp. 301–307.

James, W.D., Paris, S.W., and Malcolm, G.N. (1980) 'Study of viscous crossflow effects on circular cylinders at high Reynolds numbers', *AIAA J.*, Vol. 18, No. 9, pp. 1066-1072.

Jones, G.W., Cincotta, J.J., and Walker, R.W. (1969) 'Aerodynamics forces on a stationary and oscillating circular cylinder at high Reynolds numbers', *NASA Technical Report,* NASA TR R-300.

Launder, B.E. and Spalding, D.B. (1972) *Lectures in mathematical models of turbulence,* Academic Press, London, England.

Launder, B.E. and Spalding, D.B. (1974) 'The numerical computation of turbulent flows', *Comput. Meth. Appl. Mech. Eng.*, Vol. 3, pp. 269-289.

Menter, F.R. (1994) 'Two-equation eddy-viscosity turbulence models for engineering application', *AIAA J.*, Vol. 32, No. 8, pp. 1598-1605.

Ong, M.C., Utnes, T., Holmedal, L.E., Myrhaug, D., and Pettersen, B. (2009) 'Numerical simulation of flow around a smooth circular cylinder at very high Reynolds numbers', *Marine Struct.*, Vol. 22, pp. 142-153.

Pang, L.J.A, Skote, M., and Lim, S.Y. (2013) 'Turbulence Modeling Around Extremely Large Cylindrical Bluff Bodies', *Proc. 23th International Ocean and Polar Engineering Conference,* Vol. 1, pp. 250-256.

Patankar, S.V. and Spalding, D.B. (1972) 'A calculation procedure for heat, mass and momentum transfer in three-dimensional parabolic flows', *Int. J. of Heat and Mass Transfer,* Vol. 15, No. 10, pp. 1787-1806.

Roshko, A. (1961) 'Experiments on the flow past a circular cylinder at very high Reynolds number', *J. Fluid Mech.,* Vol. 10, No. 3, pp. 345-356.

Schewe, G. (1983) 'On the force fluctuations acting on a circular cylinder in crossflow from subcritical up to transcritical Reynolds numbers', *J. Fluid Mech.,* Vol. 133**,** pp. 265.

Schmidt, L.V. (1966) 'Fluctuating force measurements upon a circular cylinder at Reynolds number up to 5×10^6', *NASA Technical Report*, Document ID 19660022955.

Shih, T.H., Liou, W.W., Shabbir, A., Yang, Z. and Zhu, J. (1995) 'A new k-ε eddy-viscosity model for high Reynolds number turbulent flows – Model development and validation', *Computers & Fluids*, Vol. 24, No. 3, pp. 227-238.

Shih, W. C. L., Wang, C., Coles, D. and Roshko, A. (1993) 'Experiments on Flow Past Rough circular cylinders at large Reynolds numbers', *J. Wind Eng. Ind. Aerod.,* Vol. 49**,** pp. 351-368.

Smirnov, P.E. and Menter, F.R. (2009) 'Sensitization of the SST turbulence model to rotation and curvature by applying the Spalart–Shur correction term', *J Turbomach.,* Vol. 131**,** pp. 041010.

Spalart, P.R. and Shur, M. (1997) 'On the sensitization of turbulence models to rotation and curvature', *Aerosp. Sci. Technol*., Vol. 1**,** pp. 297-302.

Yakhot, V. and Orszag, S.A. (1986) 'Renormalization group analysis of turbulence: I. Basic Theory', *J. Sci. Comput*., Vol. 1,No. 1, pp. 3-51.